



PONTIFICIA UNIVERSIDAD CATOLICA DE CHILE
ESCUELA DE INGENIERIA

**CONSIDERING TEMPERATURES IN WINE
SHIPPING DECISIONS: MODEL, RISKS
INDICES, AND APPLICATIONS IN EMERGING
MARKETS**

MAX GARAFULIC

Thesis submitted to the Office of Research and Graduate Studies in partial fulfillment of the requirements for the Degree of Master of Science in Engineering (or Doctor in Engineering Sciences)

Advisor:

ALEJANDRO F. MAC CAWLEY

Santiago de Chile, (January, 2019)

© 2019, Alejandro F. Mac Cawley, Max Garafulic



PONTIFICIA UNIVERSIDAD CATOLICA DE CHILE
ESCUELA DE INGENIERIA

CONSIDERING TEMPERATURES IN WINE SHIPPING DECISIONS: MODEL, RISKS INDICES, AND APPLICATIONS IN EMERGING MARKETS

MAX GARAFULIC

Members of the Committee:

ALEJANDRO F. MAC CAWLEY

SERGIO D. MATURANA

MAURICIO A. VARAS

MARCOS E. SEPÚLVEDA

Thesis submitted to the Office of Research and Graduate Studies in partial fulfillment of the requirements for the Degree of Master of Science in Engineering (o Doctor in Engineering Sciences)

Santiago de Chile, (January, 2019)

To my parents, Viviana and Max, to
my brother, Alex, and to María.

*Because everything I am is for you.
You gave me everything, without
expecting anything in turn.*

AKNOWLEDGEMENTS

I want to thank my school, Instituto Alonso de Ercilla, where I was educated for thirteen years, and from which I have beautiful childhood memories. In particular, I want to thank my teachers, who always motivated me to study and give my best.

I am grateful to Engineering School of Pontificia Universidad Católica de Chile. Although it was never easy for me, I appreciate its exemplary demand, the quality of its teachers and their teaching. It was there where I could develop all my abilities to the maximum. Especially, I want to thank my advisor, Alejandro, who always helped and supported me during the development of this work. What I value most about Alejandro is his ability to resolve: before any doubt or difficulty that I had, he always proposed a quick and simple solution. I hope, during my professional development, to acquire that ability to find in the simplest, the best solution. I also want to thank him for the trust he placed in me by proposing to work with him as an operations consultant. I would like to thank other teacher who, without their teachings, the development of this work would have been much more difficult. I thank Ricardo Olea, from the Mathematics School, who gave me the fundamental bases that allowed me to learn everything I know about statistics and its applications. I appreciate his passion and desire to teach, always with the best attitude to help me with all my doubts.

Finally, I want to thank my family. First, to my parents, Viviana and Max, who gave their maximum effort to give me the best education and a full and happy life. Everything I am is thanks to you, and this work is also yours. Secondly, to my brother, who has been my life partner since I was three years old. Third, to my grandmother María, my best memory of childhood. I am sure that she is happy in heaven to see her grandchild as an adult. Finally, I thank the special people that surround my life: my university friends and my great life friends, “the F. band”, especially Cristian, who helped me in the indicated moment, and Gabriela, who always supported me in my best and worst moments.

TABLE OF CONTENTS

	Pag.
DEDICATION.....	iii
AKNOWLEDGEMENTS.....	iv
LIST OF FIGURES	vii
LIST OF TABLES.....	viii
RESUMEN.....	ix
ABSTRACT	x
1. INTRODUCTION	1
2. LITERATURE REVIEW.....	3
3. METHODOLOGY	6
3.1 Containers temperature data	6
3.2 External temperature data and correlations calculation	10
3.3 Regression model: fitting and validation	13
3.4 Arrhenius equation.....	14
3.5 Indicators and risk definition.....	15
4. RESULTS.....	18
4.1 Correlations and fitted model	18
4.2 Model validation	20
4.3 Decision making	22
4.3.1 Case study 1: Melbourne (AUS) – Oakland (USA)	23
4.3.2 Case study 2: Melbourne (AUS) – Miami (USA)	25
4.3.3 Case study 2: Route risk index analysis	28
5. DISCUSSION.....	30
6. CONCLUSION.....	32

REFERENCES35

APPENDIX: INTERPOLATION ALGORITHM EXPLANATION41

LIST OF FIGURES

	Pag.
Figure 1: Marked points along a San Antonio (CHI) - New York (USA) route (Mercator projection). Source: QGIS 2.18.15.	7
Figure 2: Interpolation algorithm pseudocode. Source: MiKTeX 2.9.	9
Figure 3: Application of interpolation algorithm on the example route (Mercator projection). Source: QGIS 2.18.15.	10
Figure 4: Flow chart of R commander routine.	11
Figure 5: Points of NOAA mesh (white) and rebuilt example route (green).	12
Figure 6: Example: external and internal temperatures related to a single thermograph. ...	19
Figure 7: R^2 and MSE v/s lags of internal temperature in models (lags of y_t on horizontal axis).	20
Figure 8: Forecast and actual temperatures for trip 4 and tracking signal values.	22
Figure 9: Routes from Melbourne (AUS) to Oakland (USA) (Mercator projection). Source: QGIS 2.18.15.	23
Figure 10: Heatmaps of routes in case 1. Source: QGIS 2.18.15.	25
Figure 11: Routes from Melbourne (AUS) to Miami (USA) (Mercator projection). Source: QGIS 2.18.15.	26
Figure 12: Heatmaps of routes in case 2. Source: QGIS 2.18.15.	28
Figure 13: Colormaps of least risky and alternative routes in case 2, July. Source: R 3.4.4.	29

LIST OF TABLES

	Pag.
Table 1: Trips and devices according to routes 1-24.	13
Table 2: Statistical measures of obtained correlations.	18
Table 3: Model results.	19
Table 4: RMSE and MAD for forecast using testing data.	21
Table 5: Case 1: results for indicators and unitary costs of risk decrease.	24
Table 6: Case 2: results for indicators and unitary costs of risk decrease.	26

RESUMEN

Actualmente, Chile es el cuarto país exportador de vino del mundo. La mayor parte del vino se transporta en contenedores estándar, lo que lo expone a las condiciones de temperatura del ambiente durante su transporte marítimo, lo que puede afectar su calidad. Las decisiones de transporte se basan principalmente en los costos, y generalmente se prefiere la ruta más barata, sin considerar los riesgos potenciales de temperatura. En este estudio, desarrollamos un modelo de apoyo a las decisiones para el problema de selección de rutas de envío, teniendo en cuenta el riesgo de temperatura durante el transporte marítimo. Para lograrlo, construimos un modelo que considera la información de temperatura al interior de contenedores, obtenida de 167 dataloggers distribuidos en 74 envíos marítimos de vino, y determinamos la correlación de esta variable con la temperatura externa. Gracias a que la temperatura externa está disponible en la base de datos global NCEP-NCAR, podemos determinar la temperatura interna del contenedor de cualquier ruta de envío. También presentamos un conjunto de índices de riesgo de temperatura, que nos permite evaluar el riesgo para el vino si se envía por una ruta específica. Los resultados indican un buen rendimiento del pronóstico para nuestro modelo, con baja desviación media acumulada y bajos valores de error cuadrático medio. Validamos este modelo aplicándolo a un grupo de rutas y mostramos que la ruta de menor costo puede implicar un mayor riesgo para la calidad del vino. Por lo tanto, debe considerarse una ruta alternativa que puede ser más costosa, pero menos riesgosa.

Palabras clave: calidad del vino, temperatura, riesgo, toma de decisiones, transporte marítimo.

ABSTRACT

Chile is currently the fourth largest wine exporting country in the world. Most of the wine is transported in dry containers, exposing it to the prevailing temperature conditions during its maritime transport, which can affect its quality. Transport decisions are mostly based on costs, with the least cost route being preferred usually, without considering the potential temperature risks. In this study, we develop a decision support model for the shipping route selection problem, taking into account the temperature risk during maritime transport. To achieve this, we construct a model that considers the internal container temperature information obtained from 167 dataloggers placed on 74 shipments of wine and determines the correlation with the external temperature. Because the external temperature is available through the global NCEP-NCAR database, we can determine the internal container temperature of any shipping route. We also present a set of temperature risk indices, which allows us to assess the risk to the wine shipment for a specific route. The results indicate a good forecasting performance for our model, with low mean accumulated deviation and root mean squared error values. We validate this model by applying it to a group of routes and show that the lowest cost route can have the highest risk for wine quality. Hence, a more expensive and less risky alternative route should be considered.

Keywords: wine quality, temperature, risk, decision making, maritime transport.

1. INTRODUCTION

Chile is currently the fourth largest wine exporting country in the world, with 9.8 million hectoliters (mhl) exported in 2017. It is only surpassed by Spain with 22.1 mhl, Italy with 21.4 mhl, and France with 15.4 mhl (OIV, 2017). Wine export volumes have continuously increased. In 2016, the global export volume was 104 mhl, while in 2000 it was only 60 mhl (indicating a growth of 73.33% in 16 years) (OIV, 2017). Moreover, wine exports have become highly significant in the case of wine producing countries with a small internal market, where most of the wineries obtain their income through sales in the foreign market. In the case of Chile, 67% of the wineries revenue derives from export markets, and 30% of them obtain 90% of their income from export sales (Wickramasekera and Bianchi, 2013). Therefore, within the international wine supply chain, good maritime transport decision making by the wineries has become increasingly important.

On the other hand, the high cost of reefers, which is three times that of a dry van container (Mac Cawley, 2014), causes producers to export wine in the latter. As an example, in the case of South Africa, 80% of its wine is exported in standard 20-foot containers, while the rest is exported in reefers and 40-foot containers (Meyer, 2002). Consequently, during its maritime transport, the wine is potentially exposed to extreme environmental conditions which can affect its quality, with temperature being the most important variable to consider, according to previous research (Meyer, 2002; Butzke *et al.*, 2012; Benítez *et al.*, 2003; Chung *et al.*, 2008; Lam *et al.*, 2013; Pérez-Coello *et al.*, 2003; Recamales *et al.*, 2006; Hasnip *et al.*, 2004; Sivertsen *et al.*, 2001; Hartley, 2001). Therefore, it becomes fundamental to consider the temperatures along different routes, as well as the risk they pose for the wine quality.

The main problem is that transport decisions are currently based only on the cost of transportation. Usually, the 20 freight forwarders use the least cost route to send containers (Cullinane and Toy, 2000), without considering the risk to wine quality due

heat exposure (Mac Cawley, 2014). Previously, Butzke *et al.* (2012) pointed out the ignorance of producers, shippers, and consumers regarding this problem. As a result, according to Robert Parker (2008), between 10% and 25% of wines sold in America have been damaged by exposure to high temperatures.

Our objective is to improve and support the current maritime transport decision making by assessing the risk to wine quality associated with a route, in addition to their transportation cost. To achieve this, our first contribution is to determine if there is a correlation between the temperature inside dry van containers and the external temperature along different shipping routes for bottled wine exports, in order to develop a model and predict the internal temperature along maritime trips around the world. Our second contribution is the identification of indicators that can assess the risk of a given route, based on the predicted internal temperatures along the routes and on the Arrhenius equation, which allows us to relate the temperature with an acceleration of chemical reactions in the wine (Mac Cawley, 2014). We present two case studies in section 4.3, in which the decision maker must select one of the routes available, using a port and date of departure, and a port and date of arrival.

The thesis is structured as follows. Firstly, section 2 presents a review of the research related to this work. Subsequently, the work methodology is presented in section 3, followed by the results in section 4. Finally, a discussion on the results and the conclusions are presented in sections 5 and 6, respectively.

2. LITERATURE REVIEW

One of the main studies that has documented temperature measurements in wine transport was carried out by Mac Cawley (2014). The author registered, within a four-year period, transport temperatures of 735 trips in the entire wine supply chain, using more than 1,000 dataloggers. Subsequently, he compared the temperature behavior at various stages of the chain: land transport to the port of departure, maritime transport and transshipment, and ground transportation from the port of destination to the importer. Similar to Butzke *et al.* (2012), Mac Cawley used the Arrhenius equation to quantify the risk that temperature poses to the quality of wine, by comparing the rate of chemical reactions at the temperatures observed, with the rate under ideal temperature conditions along maritime routes. Prior to this work, the most important research in this aspect was carried out by Butzke *et al.* (2012). The authors recorded the temperatures inside 47 standard 12-bottle cases of wine, dispatched from California to 13 destinations within the United States. Using the Arrhenius equation, the authors quantified the accumulated heat exposure of wine along land routes. On the other hand, Meyer (2002) summarized the research that was available on wine transportation temperatures in South Africa (based on recorded temperatures in various maritime trips) and the effect of heat exposure on some properties of wine. Another study was carried out by Marquez *et al.* (2012), where the temperatures of wine shipments to the United States from Australia were tracked with information recorded by 57 dataloggers between June and December 2008. The temperatures were studied in three stages: land transport in Australia to the port of origin, travel at sea, and transportation by land in the United States. For each stage, the averages for the mean, minimum, and maximum temperatures were calculated. These authors proposed two thresholds of 25°C and 40°C, and calculated the time at which the wine was over these limits. Finally, Hartley (2001), based on Meyer's (2002) work, studied the feasibility of importing bulk wine to the United Kingdom to reduce glass waste. In this case, the difference in the effect of heat exposure between bottled

and bulk wine was studied. The author suggested that the thermal inertia of bulk wine reduces the effect of heat exposure, thus being an advantage compared to bottled wine.

With the project NCEP-NCAR Reanalysis 1 of the National Oceanic and Atmospheric Administration (NOAA) (1996), we obtained data on environmental (external) temperatures along the maritime trips studied. Various climatological variables, including the temperature on Earth's surface, have been recorded since 1948, and documented in databases (one per year). Specifically, temperature has been recorded in a point mesh of 2.5 x 2.5 degrees of latitude and longitude, with a 6-hour frequency. The data provided by this project have mainly been used in recent climatology and atmospheric science studies (Hartmann *et al.*, 2016; Varikoden and Ramesh Kumar, 2014; Jadin *et al.*, 2010; Yang *et al.*, 2016; Zhang *et al.*, 2011; Ji *et al.*, 2018). As an example, Ji *et al.* (2018) evaluated the effects of Indian Ocean's springtime sea surface temperature on the Tibetan Plateau's heat source in summer, using daily NCEP-NCAR Reanalysis data of four climatological variables, including air temperature, at 17 pressure levels, from 1979 to 2011. On the other hand, Zhang *et al.* (2016) used monthly mean NCEP-NCAR Reanalysis of five variables, including air temperature, from 1948 to 2002, with the aim of studying the interdecadal variation in the intensity of the South Asian High (anticyclone in the upper troposphere over the Tibetan Plateau), explained by the potential anomalies in these variables.

Regarding temperature modeling, there are no previous studies in the transport sector that relate the temperature inside a system (in our case, inside containers) to the outside temperature (air temperature on Earth's surface). The relationship between temperatures has been modeled in climatological and hydrological studies. Laanaya *et al.* (2017) modeled the average daily water temperature of Santie-Marguerite River (Quebec, Canada), according to the average air temperature and flow. The aim was to compare the performance of four models, including a linear regression one. Another relevant study was carried out by Bilgili (2010), who fitted three models (a linear regression model, a nonlinear regression model, and an artificial neural network) to explain the monthly soil

temperature as a function of the monthly values of air temperature and six other meteorological variables observed at the Adana meteorological station (Turkey). Lastly, a similar study was conducted by Sahoo *et al.* (2009). Based on the data from four water streams that flow into Lake Tahoe (USA), the authors compared the accuracy of three models (artificial neural network, chaotic non-linear dynamic model, and a regression model) to explain the behavior of the daily stream water temperature based on the daily air temperature and solar radiation. They studied the effect of considering different daily lags of these two explanatory variables on the forecast performance of the models.

Related to risk in wine transport, the Arrhenius equation has been used previously to assess the danger for wine quality in the works of Butzke *et al.* (2012) and Mac Cawley (2014). However, within maritime transport, the risk concept has been addressed only for hazardous products and the environmental damage that can cause by the occurrence of accidents. Various works focused on the literature review about the risk assessment can be founded. Ozbas (2013) addressed qualitative and quantitative methods for risk analysis of accidents. On the other hand, Goerdlandt and Montewka (2015), based on Aven's (2012) classification of different approaches of risk (expected cost or loss, probability of an undesirable event, and others), reviewed works since 1970 to 2014 in which these approaches have been used. Most of the works have focused on model risk caused by collisions, groundings or petroleum spills. As an example, in the work done by Douligieris *et al.* (1997), an oil maritime transport planning model was solved. The model objective was to minimize a convex combination of the operational and spill expected risks costs of the shipping routes, used to transport oil between a port of departure and other of arrival. Later, Iakovou (2001) solved a similar multiobjective planning problem for petroleum products.

3. METHODOLOGY

Firstly, the temperature values inside containers are obtained from the previous work by Mac Cawley (2014). Secondly, an explanation is provided for how the external temperature values were obtained, based on data provided by NOAA (1996), and how the correlation values between these two variables were calculated. Subsequently, the methodology used to fit and validate the model used to predict temperatures along routes is explained. The last section explains how risk indicators for wine quality were defined for the routes.

This study presents differences with respect to previous studies. Firstly, there are no studies in the transport sector addressing the relationship between internal and external temperatures, which is possible using the NCEP-NCAR data. In addition, although environmental temperature has been used as an explanatory variable, it is always in conjunction with other variables (Laanaya *et al.*, 2017; Bilgili, 2010; Sahoo *et al.*, 2009). Furthermore, in all these studies, lags of internal temperature (dependent variable) are used as explanatory variables. In our study, the internal transport temperature is used only as a function of its previous values, while the external temperature has been modeled.

3.1 Containers temperature data

The temperature data inside dry van containers were obtained from the database by Mac Cawley (2014), with measurements taken by 167 thermographs placed on 74 transport trips, during various years and dates. In this database, each measurement of the thermograph is associated with the moment at which it was recorded. The measurement frequency is defined in two hours. Further, each thermograph is linked to the ship in which it traveled, and each ship has the times of departure and arrival to destination assigned to it and the specific maritime route followed. Finally, each route is described by its length and some marked points (longitude and latitude) that define its shape. As an

example, Figure 1 shows the points marked along a route from San Antonio (CHI) to New York (USA):



Figure 1: Marked points along a San Antonio (CHI) - New York (USA) route (Mercator projection).
Source: QGIS 2.18.15.

Although information was available on the times when the measurements were recorded, the location of the ship was unknown, which is necessary to correlate the ship's position with a point on the NCEP-NCAR mesh, and thus, to assign an external temperature value. To determine these points, an interpolation algorithm with two stages was programmed. At the first stage, the accumulated distance traveled until each marked point of the route was calculated. At the second stage, a ship was assumed to travel at a constant speed along a route. Thus, if the times of departure and arrival are t_i and t_f , respectively, and the distance of the route traveled is d , then the ship's speed is calculated as $v = d/(t_f - t_i)$. This allows the estimation of the distance traveled until each instant of temperature measurement. If we have M measurement times $t_i \leq t_m \leq t_f$, $m = 1, \dots, M$, the distance traveled by the ship is $d_m = (t_m - t_i) \cdot v$.

Then, the marked points of the route between which the ship was at each measurement time t_m , can be deduced comparing d_m with the accumulated distances of the marked

points. Subsequently, the distance between the measurement point and any of the marked points can be calculated, which is noted as d_m^2 . To assign a specific position (latitude and longitude) to each recording time, it is assumed that between each pair of marked points, the ship moves, approximately, around the shortest arc that joins them. In this sense, a point q_m is determined on this arc, whose distance to the selected marked point is similar to d_m^2 . The algorithm pseudocode is presented below in Figure 2, and an explanation of this is presented in appendix section:

```

STAGE 1:
for  $p_n, n = 1, \dots, N$  do
    Calculation of distance between marked points  $p_n$  and  $p_{n-1}$  of the route, defined as  $\bar{d}_n$ 
    Calculation of accumulated distance to each marked point in route:  $\bar{D}_n = \sum_{k=1}^n \bar{d}_k$ 
end for
Speed calculation:  $v = d / (t_f - t_i)$ 

STAGE 2:
for  $t_m, m = 1, \dots, M$  do
    Calculation of accumulated distance to each measurement point  $q_m$ :  $d_m = (t_m - t_i) \cdot v$ 

    Definition of break condition:  $\text{break}_1 = \text{FALSE}$ 
     $n = 1$ 
    while  $\text{break} = \text{FALSE}$  do

        if  $\bar{D}_n \leq d_m \leq \bar{D}_{n+1}$  then
             $\text{break}_1 = \text{TRUE}$ 
        else
             $n = n + 1$ 
        end if
    end while

    if  $m \geq 2$  then

        if  $D_n \leq d_{m-1} \leq D_{n+1}$  then
            Lower extreme point definition:  $e_{n(m)} = q_{m-1}$ 
        else
            Lower extreme point definition:  $e_{n(m)} = p_n$ 
        end if
    else
        Lower extreme point definition:  $e_{n(m)} = p_n$ 
    end if

    Upper extreme point definition  $E_{n(m)} = p_{n+1}$ 
    Definition of orthodrome parameters between extreme points
    Calculation of distance between the measurement point and lower extreme point:  $d_m^2 = d_m - D_{n(m)}$ 
    Definition of initial coordinates (starting with lower extreme point):  $\phi_m = \phi_{n(m)}, \lambda_m = \lambda_{n(m)}$ 

    if  $\phi_{n(m)} < \phi_{n(m)+1}$  then
        Definition of longitude increase in each iteration:  $\Delta\phi = 10^{-4^\circ} > 0$ 
    else
        Definition of longitude increase in each iteration:  $\Delta\phi = -10^{-4^\circ} < 0$ 
    end if

    Error definition:  $\epsilon = 1$  km
    Definition of break condition:  $\text{break}_2 = \text{FALSE}$ 
    Initial longitude:  $\phi_m + \Delta\phi$ 
    while  $\text{break}_2 = \text{FALSE}$  do
        Calculation of corresponding latitude using orthodrome equation:  $\lambda_m$ 
        Calculation of orthodromic distance to lower extreme point:  $d_m^3$ 

        if  $|d_m^3 - d_m^2| < \epsilon$  then
            return  $\phi_m, \lambda_m$ 
             $\text{break}_2 = \text{TRUE}$ 
        else
            Update longitude:  $\phi_m \leftarrow \phi_m + \Delta\phi$ 
        end if
    end while
end for

```

Figure 2: Interpolation algorithm pseudocode. Source: MiKTeX 2.9.

In this way, a trip over the route previously presented in Figure 1 can be reestablished, as shown in Figure 3:



Figure 3: Application of interpolation algorithm on the example route (Mercator projection). Source: QGIS 2.18.15.

3.2 External temperature data and correlations calculation

Once the specific points of internal temperature measurement were obtained, it was necessary to associate them with external temperature values. As stated at the beginning of section 3, temperature measurements on the Earth's surface (NCEP-NCAR data) are provided by the NOAA (1996), with a 6-hour frequency. For each thermograph, the purpose was to assign an external temperature value to each internal measurement point $q = (\varphi, \lambda)$ at a time t , and subsequently, calculate the correlation coefficient between the internal and external temperature (the longitude is denoted by φ , while the latitude is denoted by λ). To achieve this, a small routine was programmed with R commander. The flow chart of the routine is as shown below in Figure 4:

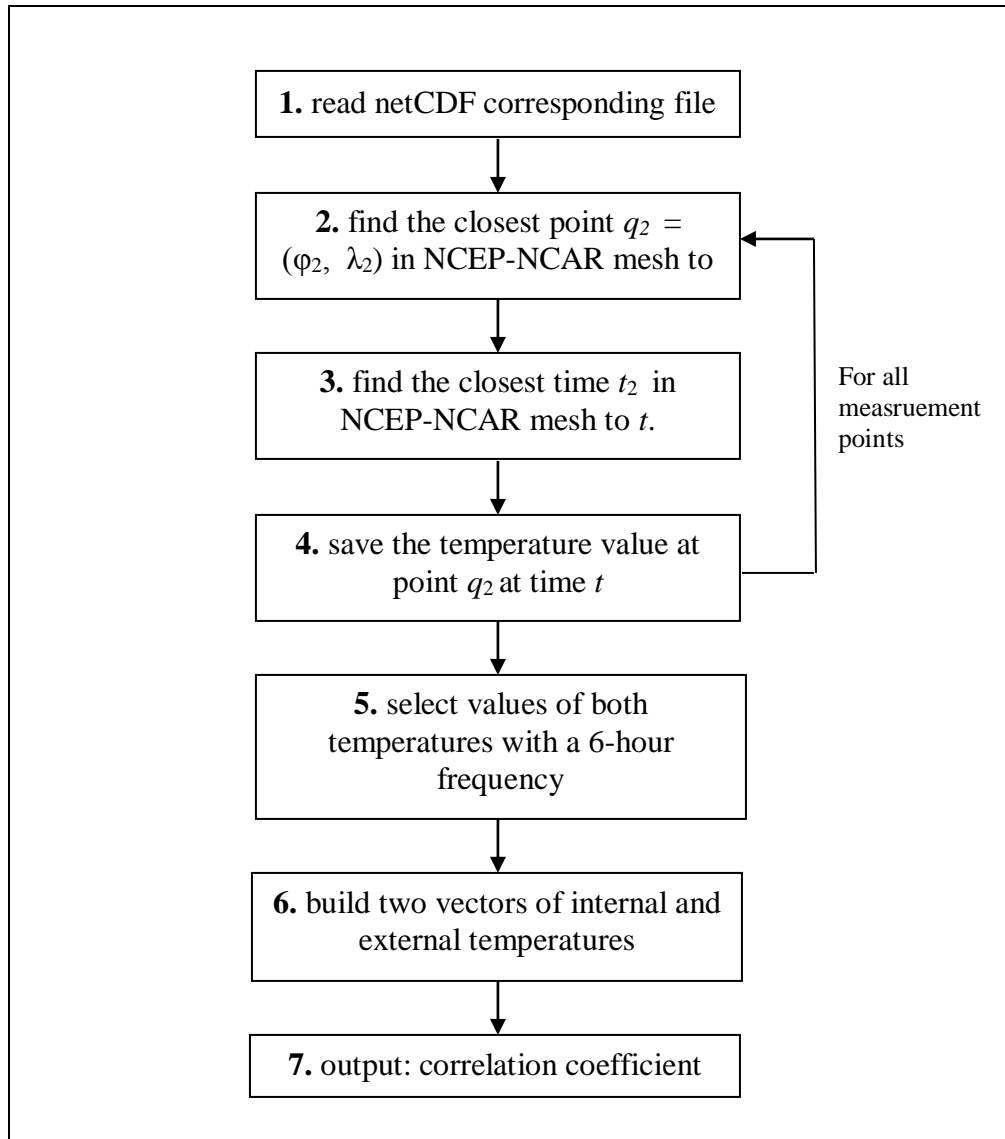


Figure 4: Flow chart of R commander routine.

In this way, the temperature values of the closest points of the NOAA mesh can be assigned to the different internal temperature measurements of the example route. The reestablished example route and the points of the NOAA mesh are shown seen below, in Figure 5:

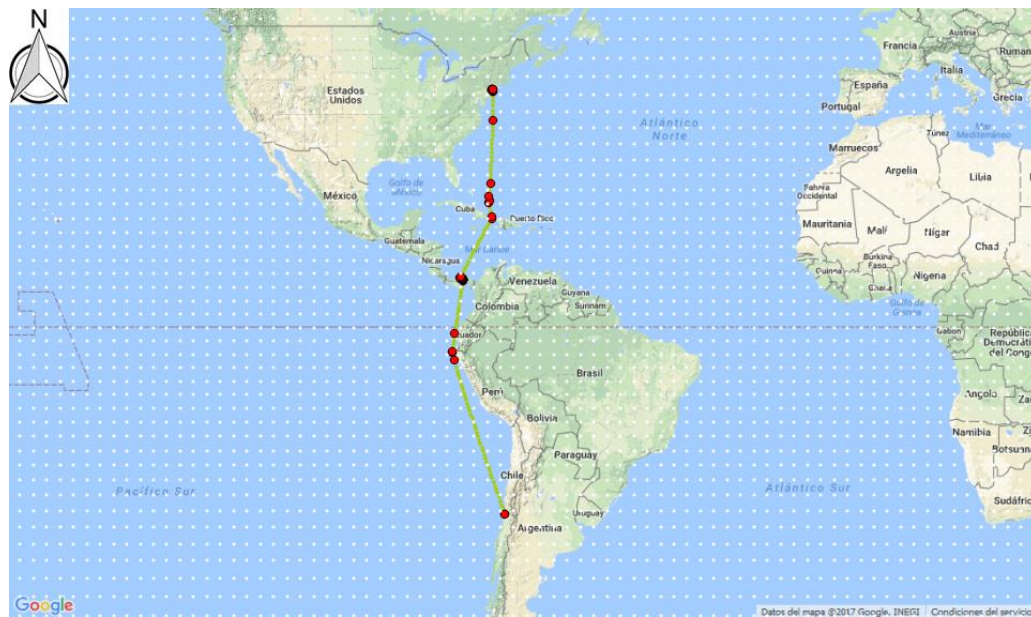


Figure 5: Points of NOAA mesh (white) and rebuilt example route (green) (Mercator Projection). Source: QGIS 2.18.15.

The correlations 145 between internal and external temperatures were calculated for each thermograph, distributed into 74 trips along 24 routes. In total, 167 correlations were calculated. The distribution of the devices and trips by route can be seen below, in Table 1:

Table 1: Trips and devices according to routes 1-24.

ID	Origin	Destiny	Trips	Devices
1	Melbourne (AUS)	Oakland (USA)	1	3
2	Valparaíso (CHI)	New York (USA)	3	15
3	San Antonio (CHI)	Charleston (USA)	1	8
4	San Antonio (CHI)	Port Elizabeth (USA)	9	18
5	San Antonio (CHI)	Houston (USA)	4	7
6	San Antonio (CHI)	Port Elizabeth (USA)	2	5
7	San Antonio (CHI)	Charleston (USA)	1	5
8	San Antonio (CHI)	Miami (USA)	6	12
9	San Antonio (CHI)	Baltimore (USA)	2	3
10	San Antonio (CHI)	Long Beach (USA)	4	5
11	San Antonio (CHI)	Port Everglades (USA)	3	7
12	San Antonio (CHI)	Baltimore (USA)	7	12
13	San Antonio (CHI)	Long Beach (USA)	1	1
14	San Antonio (CHI)	Charleston (USA)	4	5
15	San Antonio (CHI)	New York (USA)	12	33
16	San Antonio (CHI)	Port Elizabeth (USA)	1	1
17	San Antonio (CHI)	Philadelphia (USA)	3	3
18	Valparaíso (CHI)	New York (USA)	2	8
19	San Antonio (CHI)	Nola (USA)	1	1
20	San Antonio (CHI)	Nola (USA)	2	4
21	San Antonio (CHI)	Seattle (USA)	2	2
22	San Antonio (CHI)	Boston (USA)	1	2
23	Melbourne (AUS)	Miami (USA)	1	3
24	Melbourne (AUS)	Philadelphia (USA)	1	4

3.3 Regression model: fitting and validation

An autoregressive model was fitted, in which the internal temperature only depends on its previous lags and on the external temperature, that is, a model of type

$$y_t = \alpha_0 + \alpha_1 \cdot x_t + \sum_{k=1}^K \beta_k \cdot y_{t-k} + \varepsilon_t, \quad (1)$$

where y_t represents the temperature inside the containers at a time t , x_t represents the external temperature at the same time, K is the amount of internal temperature lags to

consider, and $\varepsilon_t \sim^{iid} N(0, \sigma^2)$. Each lag represents a 6-hour period. To fit the model, external temperature lags x_{t-k} were not included, as their effect is summarized in the effect of the internal temperature lags. The fitting was made with information from 65 of the 74 trips (19,097 training data), and with temperature data on Celsius scale. To select variables, the model of equation 1 was initially fitted without any internal temperature lag. Subsequently, the first lag ($K = 1$), second ($K = 2$) lag, and so on were considered, until the increase of R^2 value was observed to be insignificant.

The model was used to forecast (every 6 hours) the internal temperatures along 9 trips (2,294 test data) of various durations and during different seasons. To measure the accuracy of the forecast, two scale-dependent measures were selected: MAD, which, as Hyndman (2014) suggests, is easy to understand, and RMSE, which has been used in previous studies where the temperature is the dependent variable (Laanaya *et al.*, 2017; Sahoo *et al.*, 2009). On the other hand, unlike MAD, it penalizes errors of greater magnitude. The advantage is that these measures are in the same data scale ($^{\circ}C$). For a set of N internal temperature forecasts z_t , $t = 1, \dots, N$ and their respective realizations y_t , $t = 1, \dots, N$, the MAD and the RMSE are defined, respectively, as

$$MAD = \frac{1}{N} \cdot \sum_{t=1}^N |z_t - y_t|, \quad (2)$$

$$RMSE = \sqrt{\frac{1}{N} \cdot \sum_{t=1}^N (z_t - y_t)^2}. \quad (3)$$

3.4 Arrhenius equation

The Arrhenius equation is a mathematical expression that allows to relate the speed of a chemical reaction based on the temperature at which it occurs. In this case, the decrease in the quality of the wine, can be correlated directly with the acceleration in its chemical reactions.

The Arrhenius equation relates the constant of a chemical reaction k , with the temperature at which it occurs, according to the expression

$$k(T) = k_0 \cdot e^{-\frac{E_a}{RT}}, \quad (4)$$

where k_0 is a constant, E_a corresponds to the activation energy, measured in J/mol , R is the universal constant of the ideal gases, measured in $J^{\cdot}K^{-1}\cdot mol^{-1}$, and T is the temperature in Kelvin scale (K). Mac Cawley's method (2014) considers that the absolute increase in the speed of chemical reactions during a time t , with respect to normal temperature conditions, is given by the expression

$$\Delta v(t, T) = k_0 \cdot t \cdot e^{-\frac{E_a}{RT}} - k_0 \cdot t \cdot e^{-\frac{E_a}{RT_b}}, \quad (5)$$

which represents the difference between the speed at which the reaction occurs at a variable temperature T and the speed at which it occurs at a base temperature T_b , during a time t . As base temperature, the optimal storage temperature of wine is taken, that is, $13^{\circ}C$ (Butzke *et al.*, 2012). By calculating the quotient of the expression in equation 5 and the reaction rate under optimal conditions, that is, by $k_0 \cdot t \cdot \exp(-E_a/RT_b)$, a percentage increase in the speed of chemical reactions is obtained:

$$\begin{aligned} \% \Delta v(t, T) &= 100 \cdot \left(\frac{k_0 \cdot t \cdot e^{-\frac{E_a}{RT}} - k_0 \cdot t \cdot e^{-\frac{E_a}{RT_b}}}{k_0 \cdot t \cdot e^{-\frac{E_a}{RT_b}}} \right) \\ &= 100 \cdot \left(e^{\frac{E_a}{R} \left(\frac{1}{T_b} - \frac{1}{T} \right)} - 1 \right). \end{aligned} \quad (6)$$

By integrating equation 6 over a trip, the accumulated acceleration of chemical reactions can be quantified as percentage, denoted as Δv (%).

3.5 Indicators and risk definition

Two practical cases were studied. The aim was to indicate which of the routes is the most convenient to use in terms of risk and cost (alternative route), in case the cheapest route is not the least risky. The route risk was assessed based on the internal temperature forecast, using the model obtained in equation 1. As an external temperature forecast,

the historical means of temperatures at each point along the route are used. These are calculated based on the last 30 annual realizations until now, obtained with NCEP-NCAR database (1996).

It is assumed that the probability of the merchandise arriving in poor condition is an increasing function of three proposed indicators, considered equally important. In this way, a route risk index ρ (non dimensional) was calculated for each route, based on the percentage difference between its indicators value and the indicators value of the cheapest route. The indicators are defined as follows. Firstly, the standard deviation (variability) of internal temperatures along the trip is calculated, denoted by σ ($^{\circ}\text{C}$). According to Mac Cawley (2014), changes in temperature can cause piston movements on the corks, increasing the risk of the wine oxidation. Furthermore, a threshold of 25°C is proposed. This temperature is considered dangerous for wine quality (Mac Cawley, 2014), specially during long periods of exposure (Ough, 1992). The second indicator is the travel time τ (days) in which this threshold is exceeded. Finally, based on the Arrhenius equation and previous study of Mac Cawley (2014), the last indicator is Δv (%), defined by equation 6. As base temperature, the optimal storage temperature of wine is taken, that is, 13°C (Butzke *et al.*, 2012). The specific values of the parameters are $E_a = 41,223 \text{ J/mol}$ and $R = 8.314472 \text{ J}^{-1}\cdot\text{K}^{-1}\cdot\text{mol}^{-1}$. The value of E_a corresponds to the activation energy of starch hydrolyzed alcohol fermentation by the yeast *Saccharomyces cerevisiae*, used in wine fermentation (Mac Cawley, 2014; Converti *et al.*, 1996). As temperature values in equation 6, the temperature forecast is used. Then, if a given route and the cheapest route have indicators Δv , τ , σ and Δv_c , τ_c , σ_c , respectively, ρ (%) is defined as:

$$\rho = 100 \cdot \left(\omega_1 \cdot \frac{\Delta v_c - \Delta v}{\Delta v_c} + \omega_2 \cdot \frac{\tau_c - \tau}{\tau_c} + \omega_3 \cdot \frac{\sigma_c - \sigma}{\sigma_c} \right), \quad (7)$$

where $\omega_i = 1/3$, $i = 1, \dots, 3$. In this study, a given route is considered less risky than the cheapest route if it presents a positive ρ value. If various routes satisfy this condition, the alternative route is selected based on unitary costs, i.e. the route which presents the lowest value of the quotient of the transportation costs difference (compared with the

cheapest route) and its ρ value. This quotient is considered as the unitary (marginal) cost of risk reduction, denoted by c_ρ .

For each case analyzed, two departure dates were defined: 1 January and 1 July. Information on the services provided by different shipping companies was used to determine the travel time from the port of origin to the port of destination. With this information, arrival dates were obtained. On the other hand, maps of routes between ports are available at marinetraffic.com (2007), which provided the length and marked points that define the routes. The transportation costs of the routes were quoted in US dollars with different shipping and freight forwarders companies, based on a port-to-port service of a 20-foot dry van container, full of bottled wine (FCL). Finally, various values of the weights ω_i , $i = 1, \dots, 3$ of equation 7 were used to calculate ρ for the routes of the second case in July, with the objective of showing how risk assessment of routes and the choice of alternative routes depend on the importance assigned to each indicator.

4. RESULTS

In this section the results obtained are presented. Firstly, the correlations obtained between the internal and external temperatures and the results of the fitted model are shown. Secondly, the validation of the model and the obtained forecast error measures are presented. The last part presents the results for the application cases.

4.1 Correlations and fitted model

A total of 167 different correlations between internal temperature values and their respective external temperature values were calculated. Each correlation value was calculated based on a specific thermograph, as pointed out in section 3.1. Some statistical measures of the correlations obtained are shown in Table 2:

Table 2: Statistical measures of obtained correlations.

Indicator	Value
Min.	0.601
Mean	0.802
Median	0.814
Upper quartile	0.888
Max.	0.960

Approximately, 50% of the correlations obtained are greater than 81.4%, while 25% are higher than 88.8%. The results indicate moderate and a strong linear relationship between these variables (Ratner, 2009). As an example, a graph of the internal and external temperatures related to a single thermograph is presented in Figure 6:

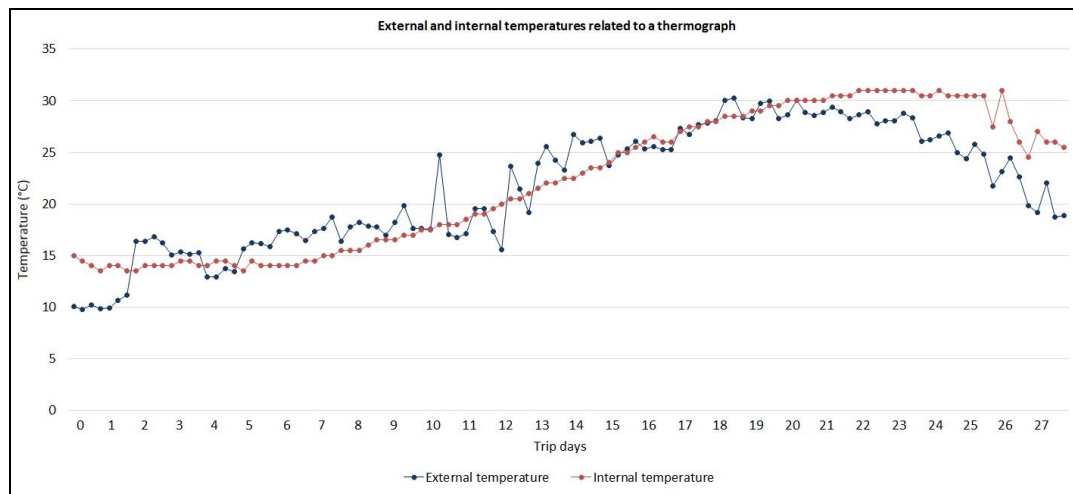


Figure 6: Example: external and internal temperatures related to a single thermograph.

In this case, the correlation value is 88.9%. As pointed out in section 3.3, to fit the model, the training data were obtained from 65 of the 74 trips. The results of the fitted model are presented in Table 3:

Table 3: Model results.

Variable	Estimator	SE	<i>t</i> value	<i>p</i> value	CI inf (95%)	CI sup (95%)
Intercept	0.0252	0.0382	0.6604	0.5090	-0.0497	0.1002
x_t	0.0348	0.0027	12.9842	0	0.0296	0.0401
y_{t-1}	0.6980	0.0066	106.4369	0	0.6852	0.7109
y_{t-2}	-0.0296	0.0067	-4.4165	0	-0.0428	-0.0165
y_{t-3}	0.1154	0.0067	17.2883	0	0.1023	0.1284
y_{t-4}	0.6445	0.0068	95.0867	0	0.6312	0.6578
y_{t-5}	-0.4643	0.0065	-71.6325	0	-0.4770	-0.4516
R^2				0.9514		
Adjusted R^2				0.9514		
RSE				1.3152		
Observations (N)				19,097		
F statistic				62,318.9430 (p value = 0)		

The internal temperature was considered up to the fifth lag ($K = 5$ in equation 1). The value obtained by R^2 indicates that the variation of y_t is explained up to 95.14% due the variation of the explanatory variables, while the high value of F statistic indicates a significant relationship between the response and the explanatory variables. An interpretation of the estimators values is provided in Section 5 (Discussion). As mentioned in section 3.3, a forward method was used to add variables to the model. Firstly, the model in equation 1 was fitted, which considers only the external temperature as a regression variable. Then, the lags of internal temperature were added until the increase in the value of R^2 was not significant. The last significant increase of R^2 occurred when the fifth lag ($K = 5$) was added. Figure 7 shows the increase in the value of R^2 and the decrease in the value of the mean of squared error (MSE) of these models:

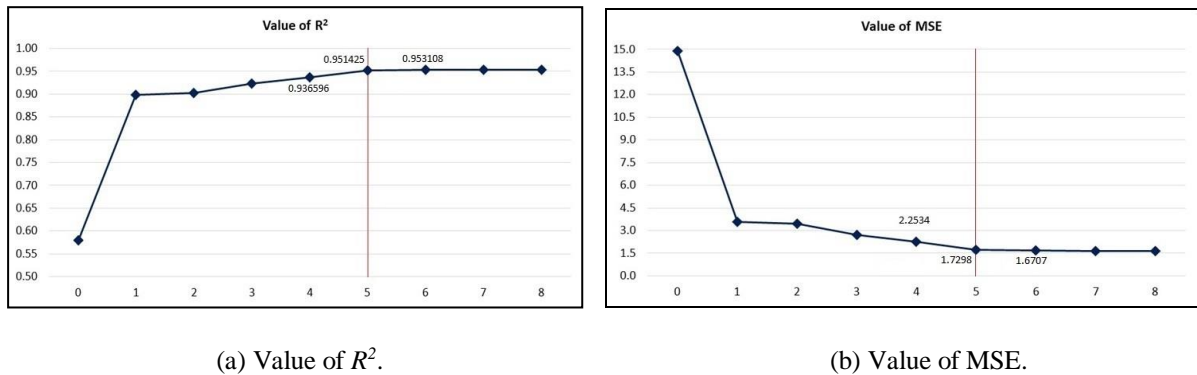


Figure 7: R^2 and MSE v/s lags of internal temperature in models (lags of y_t on horizontal axis).

4.2 Model validation

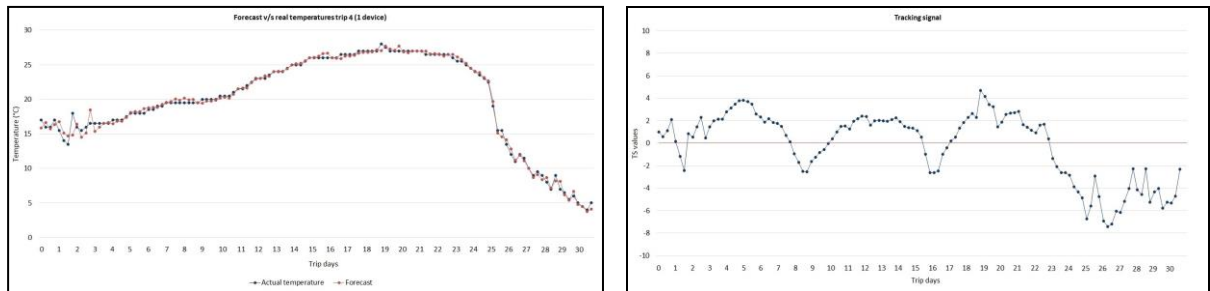
As mentioned in the section 3.3, the model was tested on 9 trips (2,294 points). The two indicators used to determine the quality of the forecast of the fitted model were MAD and RMSE. The results obtained for the accuracy of forecasts on each trip and global data (considering large vectors that link all the values of current temperatures and forecast) are presented in Table 4:

Table 4: RMSE and MAD for forecast using testing data.

Trip	RMSE (°C)	MAD (°C)
1	2.472	1.012
2	2.674	0.725
3	0.069	0.198
4	3.090	0.966
5	0.780	0.527
6	0.218	0.318
7	0.236	0.357
8	1.940	0.991
9	2.142	0.836
Global	1.425	0.805

The obtained values of RMSE are in a low-normal range, compared with those that have been obtained in research in which the temperature is predicted (Laanaya *et al.*, 2017; Gómez *et al.*, 2014). In the study by Laanaya *et al.* (2017), quoted in section 2, values ranging from 1.29°C to 2.26°C were obtained by the regression model, while its global value was 1.83°C. The best performance model had a global value of 1.44°C, higher than the global RMSE obtained by the model in this study. The performance of other meteorological models has been measured with RMSE. Gómez *et al.* (2014) obtained values ranging from 2°C to 4°C for hourly forecast temperatures of RAMS model, in 72-hour periods. The RMSE values varied according to day or night, different seasons of year, and geographic location of meteorological stations (inland or coastal), within Valencia region (Spain). The authors concluded that RAMS performance was good in spring and summer for coastal stations and in fall and winter for inland ones, with RMSE ranging from 2°C to 3°C and 2°C to 4°C, respectively. The RMSE values per trip obtained in this study are low-normal compared with this range, and the global result is significantly smaller. On the other hand, the quality of the forecast is such that, the mean absolute deviation of 1.012°C was not exceeded for any trip. The global result of MAD was 0.805°C. These results indicate that, on an average, the forecast errors are

less than 1°C . As an example, Figure 8 presents the forecast and actual temperatures recorded for trip 4, and the corresponding tracking signal:



(a) Trip 4.

(b) Tracking signal.

Figure 8: Forecast and actual temperatures for trip 4 and tracking signal values.

4.3 Decision making

The results are shown in the first two parts of this section. The aim was to indicate which route is the most convenient to use in terms of risk and cost, according to the criterion defined in section 3.5. The numeration and shape of the routes under study are shown in Figures 9 and 11, for each case, respectively. The case results are shown in Tables 5 and 6. Each table presents, for each route, the values of Δv , τ , σ , ρ (with $\omega_i = 1/3$, $i = 1, 2, 3$) and of the unitary costs of risk reduction c_p (USD/%) for each departure date, and its transportation cost (USD).

Furthermore, at the end of each case, heatmaps based on the internal temperature forecasts are presented in Figures 10 and 12. Finally, case 2, in July, was used as an example to show how different indicator weight values on ρ equation (7) affect the routes risk assessment and the choice of alternative routes. This example is presented in the last part of this section.

4.3.1 Case study 1: Melbourne (AUS) – Oakland (USA)

In this case, four routes from Melbourne (AUS) to Oakland (USA) were compared, with 35-day window. The routes studied are shown in Figure 9:

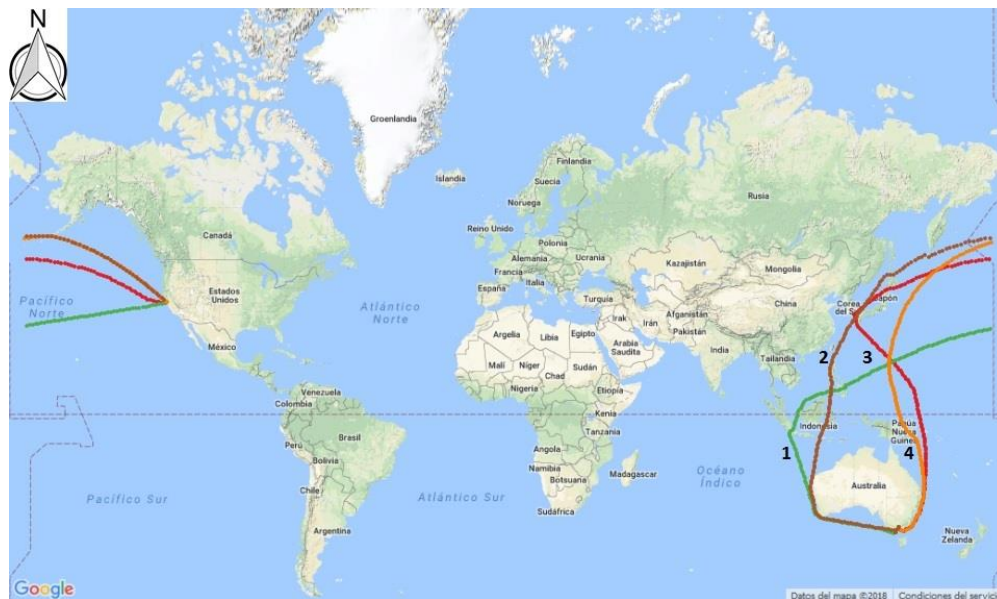


Figure 9: Routes from Melbourne (AUS) to Oakland (USA) (Mercator projection). Source: QGIS 2.18.15.

In this case, the cheapest route is route 4. The results for January and July are presented in Table 5:

Table 5: Case 1: results for indicators and unitary costs of risk decrease.

Month	Indicator/Route	1	2	3	4
January	Δv (%)	54.914	36.672	27.167	28.124
	τ (days)	0	0	2.1	1.4
	σ (°C)	3.402	7.255	7.641	7.238
	ρ (%)	19.244	23.018	-17.391	-
	c_p (USD/%)	119.518	8.689	-11.500	-
July	Δv	68.198	52.316	45.845	43.287
	τ	12.1	0.9	4.7	4
	σ	5.259	4.435	4.774	4.546
	ρ	-91.077	19.947	-9.447	-
	c_p	-48.311	10.027	-21.171	-
Cost (USD)		4,400	2,300	2,300	2,100

The following can be noted:

- **Risk results:** The values of the first two indicators increase in July for all routes, because most of their trajectory is in northern hemisphere (summer season). In January, routes 3 and 4 are less risky than routes 1 and 2 in terms of Δv . However, in terms of τ , the wine is exposed to temperatures above 25°C for 2.1 and 1.4 days, respectively. Lastly, route 1 has less variability than the others. In terms of τ , routes 1, 3 and 4 are riskier than route 2, as wine can be exposed to temperatures above 25°C for 12.1, 4.7 and 4 days, respectively. On the other hand, variability results show that route 1 is the most variable. In this sense, the σ value increases only for this route, while it decreases for routes 2 to 4. Finally, according to the route risk index ρ , the route that presents the lowest risk is route 2, for both months.
- **Alternative route:** Route 4 is the cheapest with a value of USD 2,100. Based only on cost, it should be preferred in any season. Considering the indicators as equally important, the values of ρ indicate that only route 2 should be considered, with an extra cost of USD 200, for both months. The main advantage of this route compared with the others is its low τ . The risk reduction reaches 23.018%

and 19.947%, while the costs of risk reduction are USD 8.689 and 10.027 per unit of risk percentage, for January and July, respectively. In this case, the unitary costs and the ρ values of the alternative route are similar for both months.

The heatmaps for January and July are shown in Figure 10:

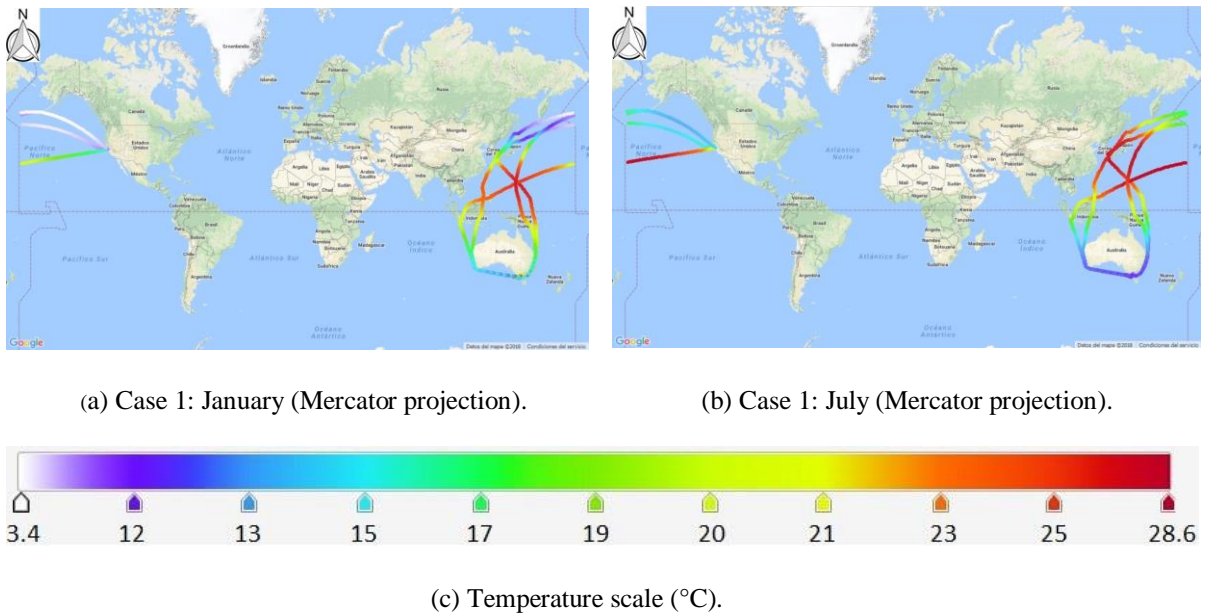


Figure 10: Heatmaps of routes in case 1. Source: QGIS 2.18.15.

4.3.2 Case study 2: Melbourne (AUS) – Miami (USA)

This case compares five routes between the ports of Melbourne (AUS) and Miami (USA) with a 40-day time window. The routes are shown in Figure 11:



Figure 11: Routes from Melbourne (AUS) to Miami (USA) (Mercator projection). Source: QGIS 2.18.15.

In this case, route 5 is the cheapest. The results for January and July can be seen in Table 6:

Table 6: Case 2: results for indicators and unitary costs of risk decrease.

Month	Indicator/Route	5	6	7	8	9
January	Δv (%)	51.412	20.763	27.655	55.276	39.731
	τ (days)	0	0	0	0	0
	σ (°C)	3.532	5.481	5.955	3.034	4.163
	ρ (%)	-	1.472	-7.470	2.193	1.612
	c_p (USD/%)	-	271.739	-53.548	729.59	434.24
July	Δv	80.849	45.348	47.521	28.924	15.116
	τ	18.8	0.2	0	2.4	0.4
	σ	5.269	3.867	3.980	4.375	5.036
	ρ	-	56.253	55.230	56.210	61.270
	c_p	-	7.111	7.242	28.465	11.425
Cost (USD)		1,900	2,300	2,300	3,500	2,600

The following can be noted:

- **Risk results:** The values of the first two indicators increase in July for the first three routes, and decrease for the others, because a significant part of the last two routes is in the southern hemisphere (winter in July). In January, routes 6 and 7 are significantly less risky than the others in terms of Δv . In terms of τ , there is no risk on any route. Lastly, route 8 has less variability than the others. In July, results for Δv show that routes 8 and 9 are the least risky, because it is summer in the northern hemisphere. In terms of τ , routes 6, 7 and 9 have no risk. Route 8 indicates 2.4 days with temperatures over the 25°C threshold, while route 5 is the most critical, with 18.8 days with temperatures over 25°C. On the other hand, variability results show that now route 5 is the most variable. In this sense, σ value increases for routes 5, 8 and 9, while it decreases for routes 6 and 7. Finally, according to ρ , route 8 poses the lowest risk in January (with a value of 2.193%), while route 9 does it in July (with a value of 61.270%).
- **Alternative route:** route 5 is the cheapest with a value of USD 1,900, and, based only on cost, it should be preferred in any season. Considering the indicators equally important, the values of ρ indicate that the only alternative is route 6, with an extra cost of USD 400, for both months. The risk decrease reaches values of 1.472% and 56.253%, while the costs of risk decrease are USD 271.739 and 7.111 per unit of risk percentage, in January and July, respectively. In this case, there is a significant risk decrease with a low unitary cost in July, while a very low risk decrease with a high unitary cost is reached in January.

The corresponding heatmaps for January and July are shown below, in Figure 12:

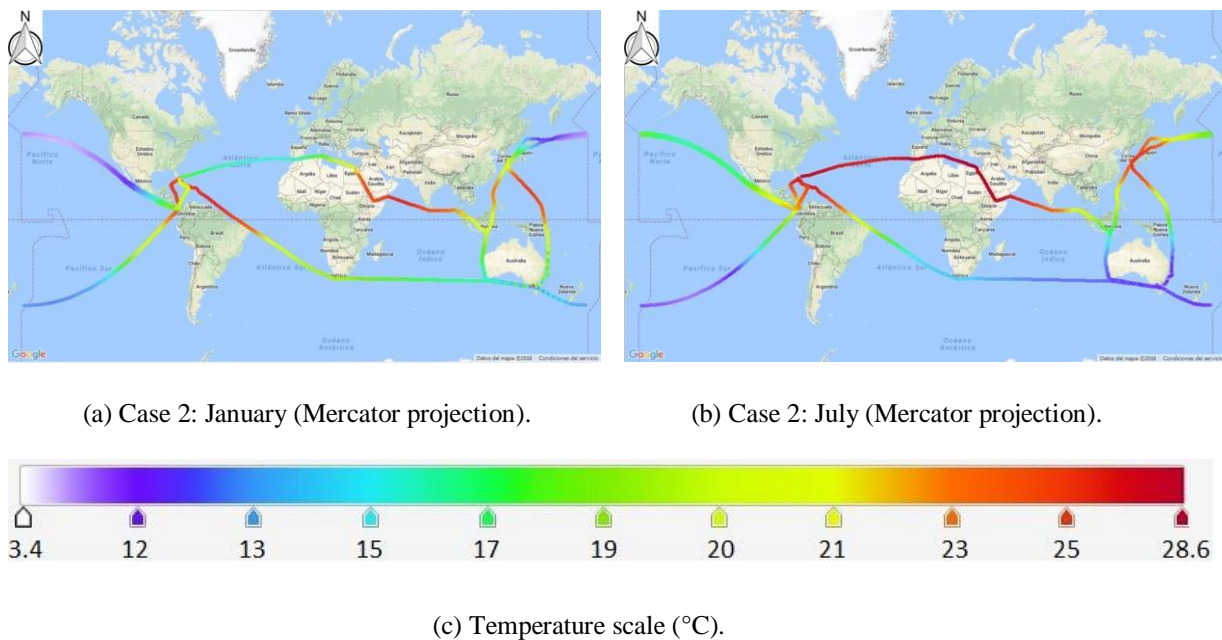
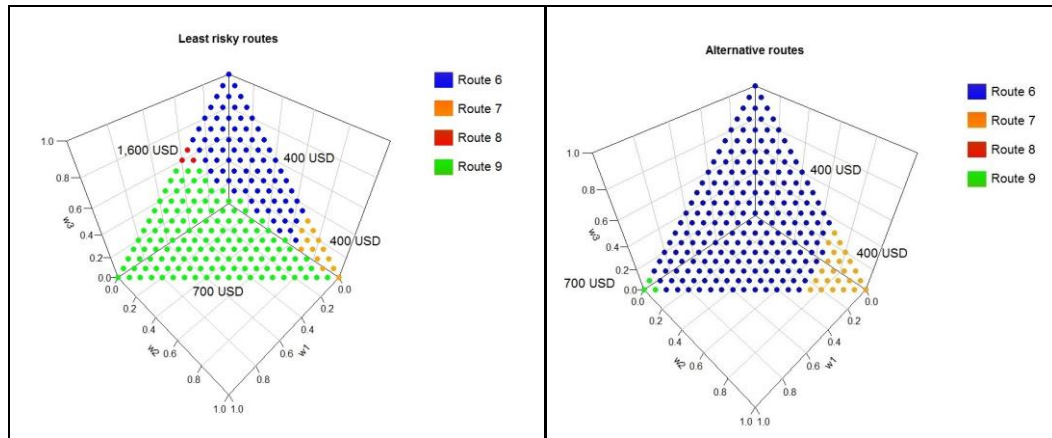


Figure 12: Heatmaps of routes in case 2. Source: QGIS 2.18.15.

4.3.3 Case study 2: Route risk index analysis

The routes risk assessment and the alternative routes of the case studies can change depending on the risk criteria, that is, the assigned relevance to each indicator, represented by changes in the indicators weights in ρ definition (equation 7). This is exemplified with case 2, in July. The analysis was carried out varying in 0.05 units the values of weights ω_1 , ω_2 and ω_3 , ranging from 0 to 1, in a lexicographical order, with the aim of generating a set of points Ω on the plane $\omega_1 + \omega_2 + \omega_3 = 1$. In this way, ρ was calculated on each point according to equation 7, and the alternative routes were defined, considering their unitary costs of risk reduction.

Figure 13 presents two colormaps for routes 6 to 9. In the first one, each color indicates the least risky route on each point of Ω . Analogously, in the second, each color indicates the most convenient route to use, instead of the cheapest, by considering the unitary costs of risk reduction:



(a) Least risky routes in case 2, July.

(b) Alternative routes in case 2, July.

Figure 13: Colormaps of least risky and alternative routes in case 2, July. Source: R 3.4.4.

With regard to most criteria, route 9 is the least risky, especially when Δv is considered highly important. On the other hand, route 6 is the least risky when σ is considered important, while the same holds true for route 7 and τ . Conversely, route 8 is considered the least risky only on a very specific combination of ω_1 , ω_2 and ω_3 .

Considering the unitary costs of risk reduction, route 6 should be selected as an alternative route for most of the criteria, as it is better than routes 8 and 9, due its low transportation cost (difference of USD 400 with the cheapest route), and consequently, its unitary cost of risk reduction. For the same reason, route 7 should be selected as an alternative instead route 9, based on high values of. Route 9 is selected only when Δv is considered highly important.

5. DISCUSSION

Results show a strong correlation between the temperature inside the containers and the outside temperature: a median of 81.4% and an upper quartile of 88.8% were obtained for the calculated correlations. This indicates that the outside temperatures have a significant effect on the inside temperatures in the case of dry van containers. It should be noted that this effect is not perfect. Therefore, it is not sufficient to know the external temperatures along a route to quantify its risk. It is necessary to correctly model the effect of the outside temperature on the temperature inside the containers.

Regarding the values of the estimators of the fitted model, it is necessary to discuss several aspects. It seems contradictory that the estimator value of α_1 is only 0.0348, because the correlation between the external and internal temperatures in all trips was greater than 0.6. This is explained by the fact that the external temperature variable loses significance in the presence of internal temperature lags. On the other hand, high estimations of β_1 (6-hour lag) and β_4 (24-hour lag) were obtained. The first value (0.6980) could be explained by thermal inertia and the effect of the most recent temperature on the current temperature. The concept of thermal inertia was studied previously by Hartley (2001). Meanwhile, the significance of the internal temperature of the previous 24 hours (value of 0.6445) can be explained by the fact that a good predictor of the next days temperature at a time t is current days temperature at the same instant. On the other hand, the estimator of β_2 is negative (-0.0296), and is explained by a "day-night" effect of the 12-hour lag temperature on the current temperature. However, the estimator values of β_3 (18-hour lag) and β_5 (30-hour lag) are not easily interpretable.

Regarding the model validation, it can be noticed that the prediction quality of the model is completely satisfactory, according to the values obtained for MAD and RMSE, as shown in Table 4. The results indicate a good forecast performance. MAD values are easily interpretable, and, with a global value of 0.805°C, are considered low for a forecast with a 6-hour frequency and over 2-week periods. The RMSE values are low-

normal compared with previous researches (Laanaya *et al.*, 2017; Gómez *et al.*, 2014), as mentioned in section 4.2, with a global value of 1.425°C.

With regard to the case study results, a seasonal behavior of the proposed indicators is observed as expected. Those routes that are mostly in the northern hemisphere, present higher values of their first two indicators during July, while they decrease in January, contrary to those that are mostly in the southern hemisphere, as shown in case 2 of section 4.3.2. In case 1 of section 4.3.1, the values of their first two indicators increase for all routes in July. With regard to σ , the reasons which explain its seasonal behavior are not clear. However, it can be noted that the value of the σ decreases for routes closer to the North Pole in July (routes 2 to 4 in case 1, and routes 6 and 7 in case 2). As a result of the indicators seasonal behavior, in terms of the route risk index ρ (with equal importance for all the indicators), the results of the case studies indicate that, in general, there is no least risky route at any time of the year. As case 2 shows, route 8 is the least risky one in January, while route 9 is the least risky in July. On the other hand, the cheapest route can be riskier for wine quality than some of the more expensive routes, as noted in both cases. Moreover, in case 2, in July, the cheapest route is always riskier than another one, according to any criterion analyzed in section 4.3.3. In this section, as shown in the first colormap of Figure 13, it is noted how the risk assessment depends on the risk criteria, and any route could be the least risky one. On the other hand, the second colormap shows how the routes transportation costs along routes become a determining factor for the choice of alternative routes: routes 6 and 7 (costs of USD 400) are preferred, instead of routes 8 and 9 (costs of USD 1,600 and 700, respectively) on points where the latter are considered the least risky routes. In this sense, the variation of ρ for each route according to various risk criteria is not sufficient to balance the difference in transportation costs: routes 6 and 7 are more similar to routes 8 and 9, based on risk instead of costs.

6. CONCLUSION

It is necessary to improve maritime transport decisions within the international supply chain, while considering the risk to wine quality due to transport temperatures. Currently, these decisions are based only on the transportation cost of the routes, with preference given to the minimum cost route between ports of origin and destination, and no consideration for the risk to wine quality.

With the objective of supporting the current transport decision making, the correlation between internal and external temperatures has been studied for the first time within the transport sector, and a simple autoregressive model of six variables has been fitted. This model allows the forecast of the temperature inside standard shipping containers (dry van) along any maritime route in the world, during any time of the year, and assigns risk indicators to each route. To achieve this, the data of temperatures inside containers were obtained from the database by Mac Cawley (2014). Subsequently, the corresponding external temperature values were assigned, based on the data provided by NOAA (1996). In this way, the correlation study and the model fitting were carried out. Once the model was validated according to the values of MAD and RMSE, it was used to calculate three proposed indicators for wine quality along various routes in two case studies, based on the predicted temperatures and the Arrhenius equation. In both cases, the routes were studied according to their indicator values and costs, to determine which route can be used instead of the cheapest route.

The obtained results indicate a moderate to strong lineal relationship (Ratner, 2009) between the internal and external temperatures, reaching correlation values over 60.1%, with a mean of 80.2%. On the other hand, the fitted model presents a great forecast performance, according to the obtained values of MAD and RMSE, with global values of 0.805°C and 1.425°C, respectively. Due the good model accuracy, the proposed indicators can be estimated with high confidence for various maritime routes.

The results of the case studies indicate that the cheapest routes can be riskier than some of the more expensive routes. It is possible to decrease the risk to wine quality significantly by using alternative routes. There is a strong seasonal behavior among the indicators. Thus, considering the seasonal factor in the route risks, there may not be a least risky route at any time of the year. Furthermore, the route risk assessment depends on the criteria, that is, the importance assigned to each indicator.

Future efforts should focus on the origin, by improving the data capture. The main limitations of this work are related to this issue. Firstly, with regard to the internal temperature measurements, although each measurement time was known, the geographical position of the ships had to be interpolated. Secondly, considering the interpolated position as the actual one, the corresponding external temperature value was assigned by determining the closest point and time in the NCEP-NCAR point mesh to the interpolated point. Consequently, the external temperature values assigned were not exact. On the other hand, the containers positions on the ships were not registered. Therefore, this was not considered a variable in the fitted model. Containers exposed directly to the sunshine can have a different internal temperature from those that are surrounded by other containers. If it is possible to register the internal and external temperatures along maritime trips, and other variables as the containers positions, the inaccuracies will be minimized and a more accurate model can be developed. Future approaches can focus on documenting the temperatures inside dry van containers and the arrival status of the merchandise in various trips, with the aim of modeling the probability $p = p(\Delta v, \tau, \sigma, \dots)$ of loss of merchandise, according to the proposed indicators and other variables, in order to define a specific risk criterion to choose alternative routes. If the value of the transported merchandise is USD V , the risk cost becomes USD $p \cdot V$. If probabilities of loss, p_c and p_a , are estimated for the cheapest and the alternative route with $p_c > p_a$ and with prices USD c_c and c_a , respectively, the latter route should be preferred if the risk cost difference is greater than the transportation cost difference, that is, if $(p_c - p_a) \cdot V > c_a - c_c$.

This work could be of interest to wineries, freight forwarders, and shipping companies. As a customer, a winery can assess the risk of the routes offered by shipping companies and freight forwarders, and improve transport decision making. As a supplier, a freight forwarder or a shipping company can offer better services by offering the customer a set of routes with various risks to wine quality.

REFERENCES

Aven, T. (2012). The risk concept-historical and recent development trends. *Reliability Engineering System Safety*, 99, 33-44.

Benítez, P., Castro, R., and García Barroso, C. (2003). Changes in the polyphenolic and volatile contents of "fino" sherry wine exposed to ultraviolet and visible radiation during storage. *Journal of Agricultural and Food Chemistry*, 51(22), 6482-6487.

Bilgili, M. (2010). Prediction of soil temperature using regression and artificial neural network models. *Meteorology and Atmospheric Physics*, 110(1), 59-70.

Butzke, C. E., Vogt, E. E., and Chacón-Rodríguez, L. (2012). Effects of heat exposure on wine quality during transport and storage. *Journal of Wine Research*, 23(1), 15-25.

Chung, H.-J. *et al.* (2008). Effect of vibration and storage on some physico-chemical properties of a commercial red wine. *Journal of Food Composition and Analysis*, 21(8), 655-659.

Converti, A., Bargaglioti, C., Cavanna, C., Nicoletta, C., and Borghi, M. D. (1996). Evaluation of kinetic parameters and thermodynamic quantities of starch hydrolysate alcohol fermentation by *saccharomyces cerevisiae*. *Bioprocess Engineering*, 15(2), 63-69.

Cullinane, K. and Toy, N. (2000). Identifying influential attributes in freight route/mode choice decisions: a content analysis. *Transportation Research Part E: Logistics and Transportation Review*, 36(1), 41-53.

Douligeris, C., Iakovou, E., and Yudhbir, L. (1997). Maritime route risk analysis for hazardous materials transportation. *IFAC Proceedings Volumes*, 30(8), 563-568.

Gómez, I., Caselles, V., and Estrela, M. (2014). Real-time weather forecasting in the western mediterranean basin: An application of the rams model. *Atmospheric Research*, 139, 71-89.

Goerlandt, F. and Montewka, J. (2015). Maritime transportation risk analysis: Review and analysis in light of some foundational issues. *Reliability Engineering System Safety*, 138, 115-134.

Hartley, A. (2001). Final report: Monitoring of wine heat exposure during commercial shipments. *Journal of Wine Research*, 23(1), 15-25.

Hartmann, H. *et al.* (2016). Seasonal predictions of precipitation in the aksu-tarim river basin for improved water resources management. *Global and Planetary Change*, 147, 86-96.

Hasnip, S. *et al.* (2004). Effects of storage time and temperature on the concentration of ethyl carbamate and its precursors in wine. *Food Additives & Contaminants*, 21(12), 1155-1161.

Hyndman, R. J., and Athanasopoulos, G. (2014). *Forecasting: principles and practice*. OTexts.com, Heathmont, Victoria.

Iakovou, E. T. (2001). An interactive multiobjective model for the strategic maritime transportation of petroleum products: risk analysis and routing. *Safety Science*, 39(1), 19-29.

Jadin, E. A. *et al.* (2010). Stratospheric wave activity and the pacific decadal oscillation. *Journal of Atmospheric and Solar-Terrestrial Physics*, 72(16), 1163-1170.

Ji, C. *et al.* (2018). On the relationship between the early spring indian ocean's sea surface temperature (sst) and the tibetan plateau atmospheric heat source in summer. *Global and Planetary Change*, 164, 1-10.

Kalnay, E. *et al.* (1996). The ncep/ncar 40-year reanalysis project. *Bulletin of the American Metereological Society*, 77, 437-470.

Laanaya, F., St-Hilaire, A., and Gloaguen, E. (2017). Water temperature modelling: comparison between the generalized additive model, logistic, residuals regression and linear regression models. *Hydrological Sciences Journal*, 62(7), 1078-1093.

Lam, H. *et al.* (2013). A real-time risk control and monitoring system for incident handling in wine storage. *Expert Systems with Applications*, 40(9), 3665-3678.

Lekkas, D. (2007). Marinetraffic. Available at: <https://www.marinetraffic.com/es/voyage-planner> (accessed August 11, 2017).

Mac Cawley, A. (2014). *The international wine supply chain: Challenges from bottling to the glass*. PhD thesis, School of Industrial and Systems Engineering. Georgia Institute of Technology.

Marquez, L. *et al.* (2012). Cool or hot: A study of containnet temperatures in australian wine shipments. *Australasian Journal of Regional Studies*, 18, 420-443.

Meyer, D. (2002). Final report: A study of the impact of shipping/transportation conditions and practices on wine. Report 1.3.1/702.0001, Technology Explotation Centre.

Organisation Internationale de la Vigne et du Vin (2017). State of the vitiviniculture world market. Technical report, Organisation Internationale de la Vigne et du Vin.

Ough, C. (1992). *Winemaking Basics*. The Haworth Press, Binghamton, NY.

Ozbas, B. (2013). Safety risk analysis of maritime transportation: Review of the literature. *Transportation Research Record*, 2326(1), 32-38.

Parker, R. (2008). *Parker's Wine Buyer's Guide: The Complete, Easy-to-use Reference on Recent Vintages, Prices, and Ratings for More Than 8,000 Wines from All the Major Wine Regions*. Simon and Schuster, New York, NY.

Pérez-Coello, M. *et al.* (2003). Influence of storage temperature on the volatile compounds of young white wines. *Food Control*, 14(5), 301-306.

Ratner, B. (2009). The correlation coefficient: Its values range between +1/-1, or do they? *Journal of Targeting, Measurement and Analysis for Marketing*, 17(2), 139-142.

Recamales, A. *et al.* (2006). The effect of time and storage conditions on the phenolic composition and colour of white wine. *Food Research International*, 39(2), 220-229.

Sahoo, G., Schladow, S., and Reuter, J. (2009). Forecasting stream water temperature using regression analysis, artificial neural network, and chaotic non-linear dynamic models. *Journal of Hydrology*, 378(3), 325-342.

Sivertsen, H. *et al.* (2001). Sensory and chemical changes in chilean cabernet sauvignon wines during storage in bottles at different temperatures. *Journal of the Science of Food and Agriculture*, 81(15), 1561-1572.

Varikoden, H. and Ramesh Kumar, M. R. and Babu, C. A. (2014). Indian summer monsoon rainfall characteristics during contrasting monsoon years. *Pure and Applied Geophysics*, 171(7), 1461-1472.

Wickramasekera, R. and Bianchi, C. C. (2013). Management characteristics and the decision to internationalize: exploration of exporters vs. non-exporters within the Chilean wine industry. *Journal of Wine Research*, 24(3), 195-209.

Yang, G., Li, C., and Tan, Y. (2016). The interdecadal variation of the intensity of the South Asian high. *Journal of Tropical Meteorology*, 22(1), 19-29.

Zhang, L., Zhi, X., and Yang, H. (2011). The relationship between the cold surge over the North Sea and the ENSO events. In *International Conference on Information Science and Technology*, pages 126-131.

APPENDICES

APPENDIX: INTERPOLATION ALGORITHM EXPLANATION

The algorithm is described as follows. Consider the representation of φ for longitude and λ for latitude. The following input is considered, given a device with M measurements during a trip, associated with:

- a maritime route with length d , marked with N points defined as $p_1 = (\varphi_1, \lambda_1), \dots, p_N = (\varphi_N, \lambda_N)$, where point p_1 corresponds to the port of origin and p_N to the port of destination,
- times of beginning and end of the trip t_i, t_f respectively, and
- times t_1, \dots, t_M of temperature measurements, ordered chronologically.

The purpose is to determine the approximate position of the ship at each measurement time $t_m, m = 1, \dots, M$. The positions to be determined are defined as points $q_m = (\varphi_m, \lambda_m), m = 1, \dots, M$. The two stages of the algorithm are as follows:

1. Stage 1:

- 1.1. Calculation of the distances between pairs of continuous points p_n and p_{n-1} along the route, defined as δ_n , with $\delta_1 = 0$.
- 1.2. Calculation of accumulated distance to each point marked along the route, defined as

$$\Delta_n = \sum_{k=1}^n \delta_k$$

- 1.3. Calculation of the ship speed, as $v = d/(t_f - t_i)$.

The second stage is executed for each searched point $q_m = (\varphi_m, \lambda_m), m = 1, \dots, M$:

2. Stage 2:

- 2.1. Calculation of the distance traveled up to the time of measurement t_m , defined as $d_m = (t_i - t_i) \cdot v$.
- 2.2. Given the distance traveled until each measurement time m , the pair of marked points along the route between the ship was located is determined. If $\Delta_n \leq d_m \leq \Delta_{n+1}$, then the ship was between the mark marked points p_n and

p_{n+1} , and p_n is defined as the lower extreme point and p_{n+1} as the upper extreme point associated to q_m . If the same condition holds true for the previous searched measurement point, that is, $\Delta_n \leq d_{m-1} \leq \Delta_{n+1}$, $m \geq 2$, then it is convenient to define the lower extreme point as q_{m-1} , which is closer to q_m . The lower and upper extreme points are denoted as $e_{n(m)}$ and $E_{n(m)}$, respectively. The extremes points are the points between the ship was, approximately, at time t_m , following the direction from the lower to the upper point.

- 2.3. The latitude λ_m and longitude φ_m of the searched point q_m are initialized as the values of the coordinates of the lower extreme point, that is, $\lambda_m = \lambda_{n(m)}$ and $\varphi_m = \varphi_{n(m)}$.
- 2.4. Calculation of the distance between the measurement point and the lower extreme point, defined as $d^2_m = d_m - \Delta_{n(m)}$.
- 2.5. The longitude of the searched point is increased by a small angle $\Delta\varphi$:
 $\varphi_m \leftarrow \varphi_m + \Delta\varphi$. This angle can be positive or negative. If the longitude of the lower extreme point is less than the longitude of the upper point, then a positive $\Delta\varphi$ is selected. Otherwise, a negative is selected. This allows considering the direction followed by the ship between the extreme points.
- 2.6. Calculation of the new point latitude $\lambda_m \leftarrow$, assuming that the point is on the orthodrome between the extreme points. The orthodrome equation is used.
- 2.7. Calculation of the distance between the obtained point $q_m = (\varphi_m, \lambda_m)$ and the point $e_{n(m)}$, defined as d^3_m , using orthodromic distances.
- 2.8. If the orthodromic distance d^3_m is similar to d^2_m , that is, if $|d^3_m - d^2_m| < \varepsilon$, then the position of the ship at the time of measurement is determined and the algorithm returns the point coordinates (a point on the orthodrome between the extreme points which distance is very similar to d^2_m was determined). ε is the error allowed. If not, it is necessary to return to point 2.4, add a new longitudinal increase $\Delta\varphi$ and execute steps 2.6, 2.7 and 2.8.